

The Impact of Sea Surface Temperature Anomalies on the Rainfall over Northeast Brazil

CARLOS R. MECHOSO

Department of Atmospheric Sciences, University of California, Los Angeles, Los Angeles, California

STEVEN W. LYONS

Department of Meteorology, Texas A&M University, College Station, Texas

JOSEPH A. SPAHR

Department of Atmospheric Sciences, University of California, Los Angeles, Los Angeles, California

(Manuscript received 13 December 1988, in final form 31 January 1990)

ABSTRACT

The response of the tropical atmosphere to the sea surface temperature (SST) anomalies in the Northern Hemisphere spring of 1984 is investigated. The methodology for investigation consists of comparing simulations with and without the global distribution of SST anomalies in the boundary conditions of the UCLA General Circulation Model (GCM). At low levels, the response includes weaker southeast trade winds over the Atlantic, increased precipitation off the northeast coast of Brazil, and reduced precipitation west of this region. The increased precipitation is due to enhanced convergence of moisture advected by the southeast trade winds, although the trades themselves are weaker. The results for the western equatorial Atlantic are in apparent agreement with the observed anomalous southern migration of the ITCZ in years with warm SST anomalies in the southern tropical Atlantic. There are strong anomalous trade winds over the Pacific extending east of the date line and weak wind anomalies over the maritime continent, in broad agreement with the observed.

The sensitivity of the simulated atmospheric response over an ocean basin to using the SST anomalies confined to the basin or in the global ocean is analyzed. It is found that there can be notable local differences in the results obtained using those procedures. In particular, the simulation with the SST anomalies confined to the Pacific shows weak anomalous trade winds over the western part of this ocean basin and strong westerly anomalies over the maritime continent unlike that with the anomalies in the global ocean.

1. Introduction

In the northeastern region of Brazil, called the Nordeste, precipitation peaks between March and May. This rainy season develops in association with the southern migration of a complex of quasi-permanent circulation features, which also affect the adjacent Atlantic Ocean (Ratisbona 1976; Hastenrath and Heller 1976; Kousky 1979). Along the eastern coast of the region, rainfall has a nocturnal maximum as the opposition of the trade winds and land-breeze enhances the convergence locally (Kousky 1979). In the southern part of the region, the precipitation also peaks during December in association with invading fronts originating from the midlatitudes of the Southern Hemisphere (Kousky and Chu 1978).

The rainfall amount over the Nordeste has strong interannual variations. Serra and Ratisbona (1942) show that anomalous southward and northward dis-

placements of the ITCZ during March and April correspond to strong and weak rainy seasons, respectively. Servain and Seva (1987) find that meridional wind stress anomalies over the tropical Atlantic and precipitation over the Nordeste are negatively correlated in the period February through May during the years 1964–1984. This means that an anomalous northward displacement of the ITCZ is associated with a decrease in precipitation over the Nordeste. In particular, the ITCZ remains north of the equator in years with drought (*secas*). In the southern part of the region, years with the greatest precipitation correspond to the largest number of frontal passages (Kousky 1979).

The observational evidence also shows correlations between anomalies in rainfall over the Nordeste and in sea surface temperature (SST) over the tropical Atlantic and Pacific oceans. [In these ocean basins, SST anomalies with significant magnitudes and large-scale patterns are a recurrent phenomenon (Lamb et al. 1986; Rasmusson and Carpenter 1982).] Hastenrath and Heller (1976) find a negative correlation between rainfall over the Nordeste and SST along the Ecuador–Peru coast. Markham and McLain (1977) find a pos-

Corresponding author address: Dr. Carlos R. Mechoso, Dept. of Atmospheric Sciences, UCLA, 405 Hilgard Avenue, Los Angeles, CA 90024.

itive lag-correlation for as early as November between the SST at locations in the tropical Atlantic and the rainfall in Ceara during the following rainy season. Such a long lag is not surprising given the persistence of SST anomalies. (They also find correlations with shorter time-lags.) Hastenrath (1978) reaffirms that *secas* are associated with anomalously high sea level pressure and cold SSTs in the southern equatorial Atlantic, low sea level pressure and warm SSTs in a band across the northern equatorial Atlantic, and warm SSTs in the tropical eastern Pacific. On the other hand, floods in the Nordeste are associated with approximately the inverse pattern of SST anomalies. Hastenrath (1984) points out that anomalously cold, south equatorial waters contribute to the development of *secas* because they are associated with a reduction of the moisture content and instability in the planetary boundary layer (PBL) upstream of the Nordeste.

The anomalies in precipitation over the Nordeste, therefore, are related to anomalies in both SST in the tropical oceans and displacement of the ITCZ, which can themselves be related. In this paper, we investigate the mechanisms involved in the connection between these atmospheric and oceanic anomalies.

The pattern of SST anomalies in the tropical Pacific is characterized by variations in the zonal direction: warm or cold anomalies develop in the eastern part of the basin (e.g., Rasmusson and Carpenter 1982). In contrast, the pattern of SST anomalies over the tropical Atlantic is characterized by variations in the meridional direction (Philander 1986). Since convection tends to be more active over warm surface waters, SST anomalies in the tropical Pacific and Atlantic are associated with zonal and meridional displacements in anomalous precipitation over the corresponding ocean basins: years with warm or cold SST anomalies in the southern equatorial Atlantic show an ITCZ displaced southward or northward of its climatological position, respectively.

There are not many general circulation model (GCM) studies on the sensitivity of the precipitation over the Brazilian Nordeste to SST anomalies in the tropical Atlantic. In principle, the generally coarse resolution of GCMs used in SST sensitivity studies does not promise illuminating results for the circulation over such a small geographical area. Nevertheless, the existing studies show encouraging results for the large-scale pattern of the circulation anomalies. An excellent example is the study by Moura and Shukla (1981). They use an idealization of the observed distribution of SST anomalies for years of *secas*. Their results confirm that the SST anomalies result in reduced precipitation over the western equatorial Atlantic in an area of enhanced sinking motion.

Mechoso and Lyons (1988; hereafter called ML) investigate the impact of SST anomalies observed during the Northern Hemisphere (NH) springs of 1984 and 1983 on the atmospheric circulation over the tropical Atlantic and Pacific. The most dramatic event of

anomalous SST on record occurs in the tropical Atlantic in 1984 after the most intense El Niño event on record in the Pacific (Servain and Sela 1987). In the tropical Atlantic during the NH spring of 1984, intense, warm SST anomalies prevail south of the equator with local maxima along the coasts of South America and Africa, and there are cold SST anomalies along the northern coast of South America. Except for the eastern coast of Brazil where there are weak positive values, the pattern of SST anomalies during the NH spring of 1983 is nearly opposite to that in 1984.

ML compares results obtained in multiyear simulations using the UCLA GCM with and without the observed anomalies in the prescribed distribution of SST (anomaly and control simulations, respectively). All other boundary conditions prescribed for the simulations, as well as the initial conditions, are identical in the anomaly and control. In this respect, the GCM constitutes a controlled environment to study the impact of SST anomalies on the atmospheric circulation.

The comparison performed in ML between the control and anomaly simulations for the period corresponding to the NH spring of 1984 shows circulation anomalies with large-scale patterns. For low levels, there is a weakened anticyclonic circulation over southeast Brazil with anomalous westerlies over the equatorial Atlantic, and there are easterlies over the equatorial Pacific and western South America. In association with the wind anomalies, there is anomalous convergence and enhanced precipitation off the coast of the Nordeste, and anomalous divergence and reduced precipitation off the northern coast of Brazil. These simulated anomalies are in broad agreement with the observed (Horel et al. 1986). The agreement suggests that the circulation anomalies observed during the NH spring of 1984 over the tropical Atlantic and Pacific are primarily due to the SST anomalies.

In this paper, we re-examine the problem posed in ML and extend that study in two major directions. First, we analyze in more detail the impact of SST anomalies in the tropical Atlantic on the atmospheric circulation. Second, we investigate the nonlinearities and remote effects in the atmospheric response to SST anomalies. Since ML uses global distributions of observed SST anomalies, the question arises as to whether it might suffice to use the anomalies confined to the Atlantic. To answer this question, we compare simulations with the UCLA GCM in which the prescribed boundary conditions for SST include or exclude SST anomalies observed over the global ocean or over a single ocean basin. We concentrate on the tropics, where significant results are obtained with a small number of simulations.

We begin in section 2 by describing the simulations performed for this study. In section 3, we present the simulated response of the atmospheric circulation to distributions of SST anomalies differing in their geographical extent. In section 4, we analyze the simulated

anomalies in precipitation and moisture flux. Section 5 focuses on the nonlinearity and teleconnections in the response of the atmosphere to SST anomalies. A brief discussion on the diurnal variation of anomalous precipitation is included in section 6.

2. The simulations performed for this study

The major characteristics of the UCLA GCM are described in ML, and more detailed descriptions are referenced therein. For this study, we use the low-resolution (5° longitude by 4° latitude), 9-layer version. In the GCM, the SST distributions are prescribed at midmonth, and intermediate distributions are obtained by linear interpolation. The SST distributions used in the simulations are obtained from the monthly mean fields of observed anomalies and climatology compiled by the U.S. National Meteorological Center (NMC). In the anomaly simulations, the SST anomalies are superimposed on the climatology. In the control simulation, the SST distributions correspond to the climatology.

The simulation with the global distribution of SST anomalies, as well as the control simulation, start from initial conditions corresponding to those observed on 1200 UTC 1 October 1982 and end three years later. We perform three additional simulations with the SST anomalies confined to the Atlantic, Pacific, and Indian oceans, respectively (see Fig. 1). These start from initial conditions corresponding to 0000 UTC 1 January 1984 in the simulation with the global distribution of observed SST anomalies and end five months later. The analysis period corresponding to the NH spring (March–May) of 1984, therefore, is beyond the range

of deterministic predictability in all cases and comparison between instantaneous fields and observations is not meaningful. Accordingly, our analysis focuses on NH spring-mean fields.

The notation used in this paper to identify the simulations is as follows:

i) CSC: control spring climatology, which is defined as the mean of the three NH springs (1983, 1984, 1985) in the control simulation.

ii) ASG4 and ASG3: simulations for the periods corresponding to the NH springs of 1984 and 1983, respectively, with the global distribution of SST anomalies.

iii) ASA4, ASP4, and ASI4: simulations for the period corresponding to the NH spring of 1984 with the SST anomalies confined to the Atlantic, Pacific, and Indian oceans, respectively.

The results presented in this paper are organized as longitude–latitude maps for the latitude band 30°S – 30°N . We define anomaly field as the result of subtracting the corresponding field in CSC from that obtained in an anomaly simulation. We define difference field as the results of subtracting the corresponding fields obtained in two different periods of either the anomaly or control simulations.

The SST anomalies observed in the tropics during April 1983 and April 1984 are shown in Fig. 2. During April 1983, there are large positive SST anomalies along the eastern equatorial Pacific in association with the decaying phase of El Niño, with highest values along the coast of Peru. There are weak positive anomalies in the entire Atlantic, except along the coast of Africa in the Southern Hemisphere. This pattern differs

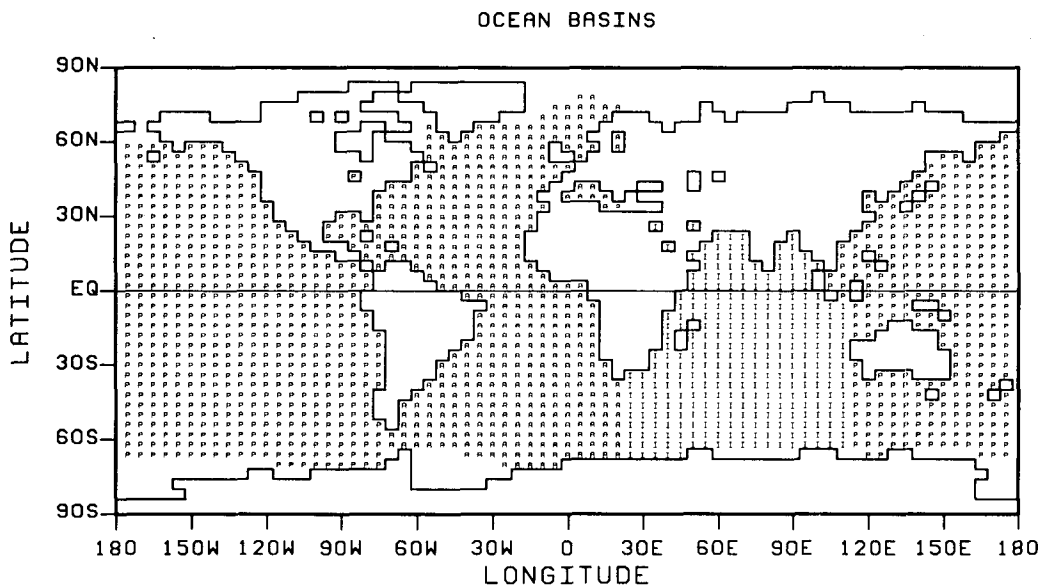


FIG. 1. The regions referred in the text as Atlantic, Pacific, and Indian oceans (A, P, and I, respectively). The unlabeled ocean regions correspond to the prescribed sea-ice for April.

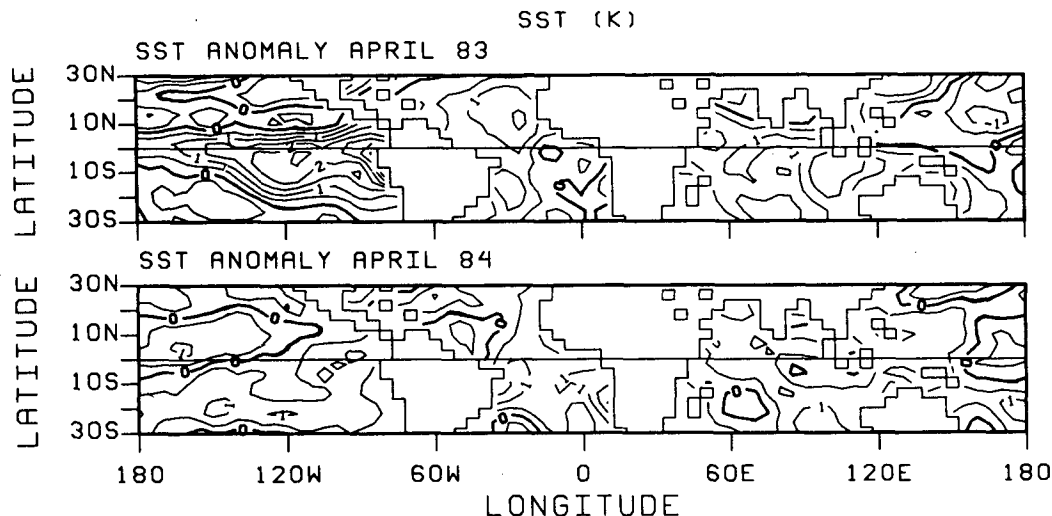


FIG. 2. The SST anomalies (K) observed in April 1983 and April 1984. Contour interval: 0.5 K.

markedly from the corresponding pattern in 1984. During April 1984, there are still positive anomalies in the eastern equatorial Pacific, but there are negative anomalies along the central and western equatorial Pacific. There are negative and positive anomalies along the coast of South America in the northern and southern equatorial Atlantic, respectively. There are also intense positive anomalies in the south Atlantic along the coast of Africa. The Atlantic pattern for April 1984 and that used by Moura and Shukla (1981) are nearly opposite. There are positive SST anomalies in the Indian Ocean in both 1984 and 1983.

3. Simulated wind anomalies

The NH spring-mean for 1984 of the rotational wind and streamfunction anomalies are shown in Fig. 3. At 850 mb, the rotational wind anomalies obtained with the global distribution of SST (ASG4-CSC) are strong over the tropics. There are anomalous westerlies over the Atlantic and Indian oceans, as well as over South America, Africa, and northern Australia, and easterlies over the equatorial Pacific. The anomalous westerlies are associated with a weakening of the subtropical highs over the South Atlantic and Indian oceans. The anomalous easterlies, which are strongest over the western Pacific, are primarily associated with a strengthening of the subtropical highs over the Pacific in both hemispheres. The rotational wind anomalies at 200 mb (not shown) generally have directions opposite to those at 850 mb. All of these simulated anomalies are in good agreement with the observed (see *Climate Analysis Bulletin*, NOAA/NMC, May 1984), but their magnitudes at 200 mb are generally weaker than the observed.

Figure 3 shows that the NH spring-mean rotational wind and streamfunction anomalies obtained with the

SST anomalies confined to a single ocean basin are only locally similar to those obtained with the global distribution of SST anomalies. At 850 mb, the rotational wind anomalies obtained in ASA4 and ASG4 are similar only over equatorial South America and the western equatorial Atlantic. Consistently, there is only one clearly defined center of anomalous cyclonic circulation in the subtropics of the Southern Hemisphere. Over Africa, the region of anomalous westerlies is displaced southward compared to ASG4. In both ASP4 and ASG4 there are anomalous easterlies over the western equatorial Pacific—although with substantially weaker magnitudes in the former than in the latter simulation—and westerlies over the eastern Indian Ocean. On the other hand, the wind anomalies obtained over the central equatorial Pacific are very different: there are anomalous westerlies in ASP4 and easterlies in ASG4. Also, wind anomalies over the maritime continent are strong and westerly in ASP4, and weak in ASG4. The wind anomalies obtained in ASI4 and ASG4 are generally similar in direction; the agreement over the tropical Pacific is particularly interesting. However, they are comparable in magnitude only over the Indian Ocean and equatorial Africa.

We now take a more detailed look at the differences over the Pacific between the wind anomalies obtained in ASG4 and ASP4. A longitude-time contour plot of 15-day running, mean zonal wind anomalies over the equator at 850 mb is shown in Fig. 4. Over the western Pacific, negative anomalies persist throughout the period in both ASG4 and ASP4, but their magnitude is stronger in the former than in the latter simulation. Over the central Pacific, on the other hand, the anomalies are mostly negative in ASG4 and positive in ASP4, the latter anomalies becoming stronger toward the end of the period. Over the maritime continent, positive and negative anomalies in ASG4 alternate in time dur-

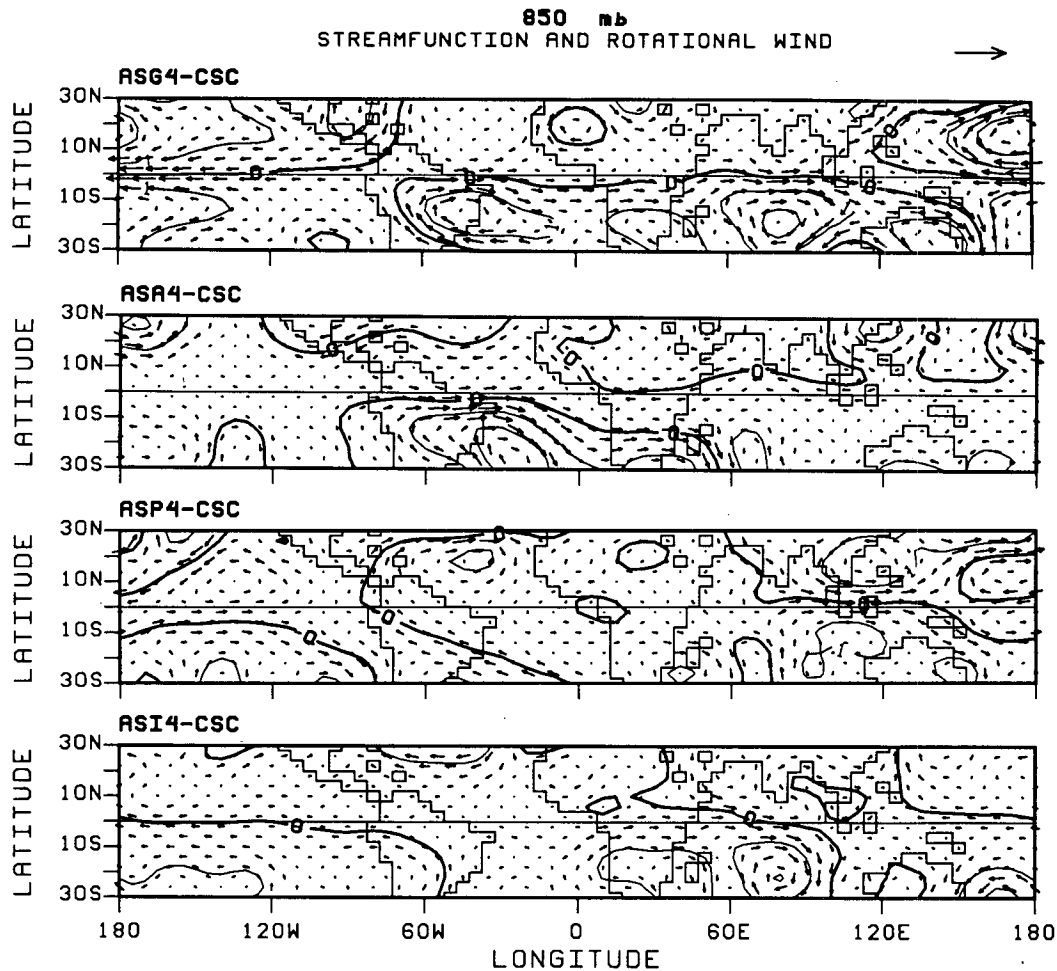


FIG. 3. From top to bottom: NH spring-mean for 1984 of the rotational wind and streamfunction anomalies obtained in the simulations with the SST anomalies for the Global, Atlantic, Pacific and Indian oceans. Reference arrow: 4 m s^{-1} . Contour interval: $1.0 \times 10^6 \text{ m}^2 \text{ s}^{-1}$.

ing the first half of the period, before becoming mostly negative during the second half; the corresponding anomalies in ASP4 are strong and positive throughout the period. Figure 4 clarifies, therefore, that anomalies in the equatorial Pacific shown in Fig. 3 for both ASG4 and ASP4 are not crucially dependent on the values during a subperiod; rather, they are representative of the entire period.

Philander (1986) points out that the trade winds over the central and western Pacific are stronger than normal during 1984. He questions whether this strengthening is due to the cold SST anomalies in the tropical sector of the Pacific Ocean. Our results give a negative answer to this question: the strengthening in question is an integral part of the atmospheric response to the global SST anomaly field, and is not obtained with the component of the field corresponding to the single ocean basin. The sensitivity of these results to the starting date of the simulations is discussed in the Appendix.

In order to assess the impact of SST anomalies on the simulated interannual variability of the tropical circulation, we plot in Fig. 5 the difference between streamfunction and rotational wind fields corresponding to two NH springs (1984 and 1983), as obtained in the simulation with the global distribution of SST anomalies and in the control simulation. In the anomaly simulations, there are large easterly differences over the Pacific. This is expected, since the SST anomalies during 1983 include El Niño. The differences over the Atlantic and Indian oceans are very similar to the anomalies obtained in ASG4. On the other hand, the differences between consecutive springs in the control simulation are small and do not exhibit an organized pattern. We obtain qualitatively the same results for all other simulated fields. If the observed SST anomalies are included in the GCM, then the simulated interannual variability of the tropical atmospheric circulation is greatly enhanced.

The NH spring-mean for 1984 of the divergent wind

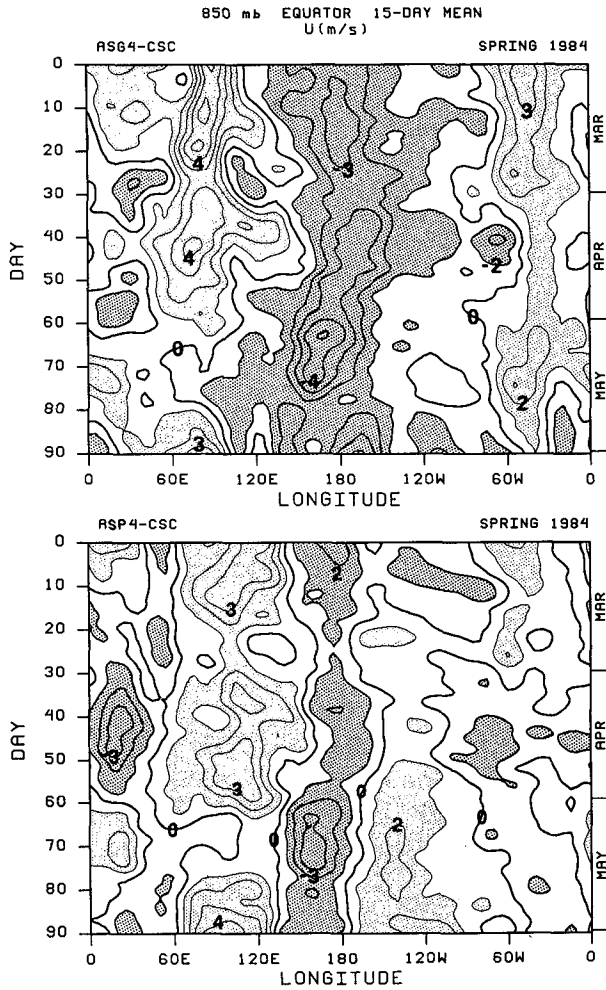


FIG. 4. Longitude-time contour plot of 15-day mean zonal wind anomalies over the equator at 850 mb. Contour interval: 1 m s^{-1} .

and velocity potential anomalies are shown in Fig. 6. At 850 mb, the divergent wind anomalies in ASG4 include westerlies over eastern South America, Africa, and the Indian Ocean, and easterlies over the western Pacific. Accordingly, there is anomalous convergence over the western Atlantic, west Indian Ocean and maritime continent, and anomalous divergence over equatorial central South America, and central Pacific. The divergent wind anomalies in ASA4 are similar to those in ASG4 over the Atlantic and are small everywhere else except over the central Pacific where they are westerly and part of a weak divergence-convergence dipole without counterpart in ASG4. The divergent wind anomalies in ASP4 are significant only over the Pacific. Here, there is anomalous convergence over the western part (as ASG4) and over the eastern part (unlike ASG4). The divergent wind anomalies in ASI4 resemble those in ASG4 over Africa and the Indian Ocean, and are small over other regions.

4. Simulated precipitation and moisture flux convergence anomalies

The NH spring-mean climatological precipitation obtained in the control simulation is shown in Fig. 7 (CSC). There are continental maxima over the Amazon and equatorial Africa, and hints of the ITCZ over the tropical oceans with the blurring expected from the relatively coarse resolution used in the GCM. There is also a South Pacific convergence zone (SPCZ) and local maxima over the islands of the maritime continent. The anomalous precipitation obtained in the SST sensitivity experiments is also shown in Fig. 7. The most outstanding features obtained in ASG4 are the region of enhanced precipitation northeast of Indonesia and the dipole of reduced precipitation over northern Brazil

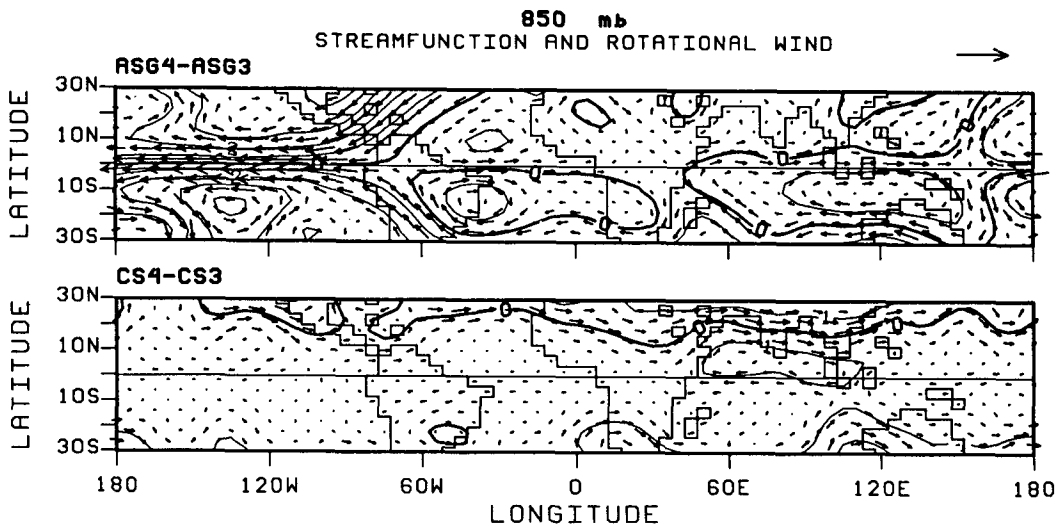


FIG. 5. From top to bottom: Differences between the NH spring-mean for 1984 and 1983 of the rotational wind and streamfunction obtained in the anomaly simulation with the global distribution of SST anomalies (top) and in the control simulation (bottom). Reference arrow: 4 m s^{-1} . Contour interval: $1.0 \times 10^6 \text{ m}^2 \text{ s}^{-1}$.

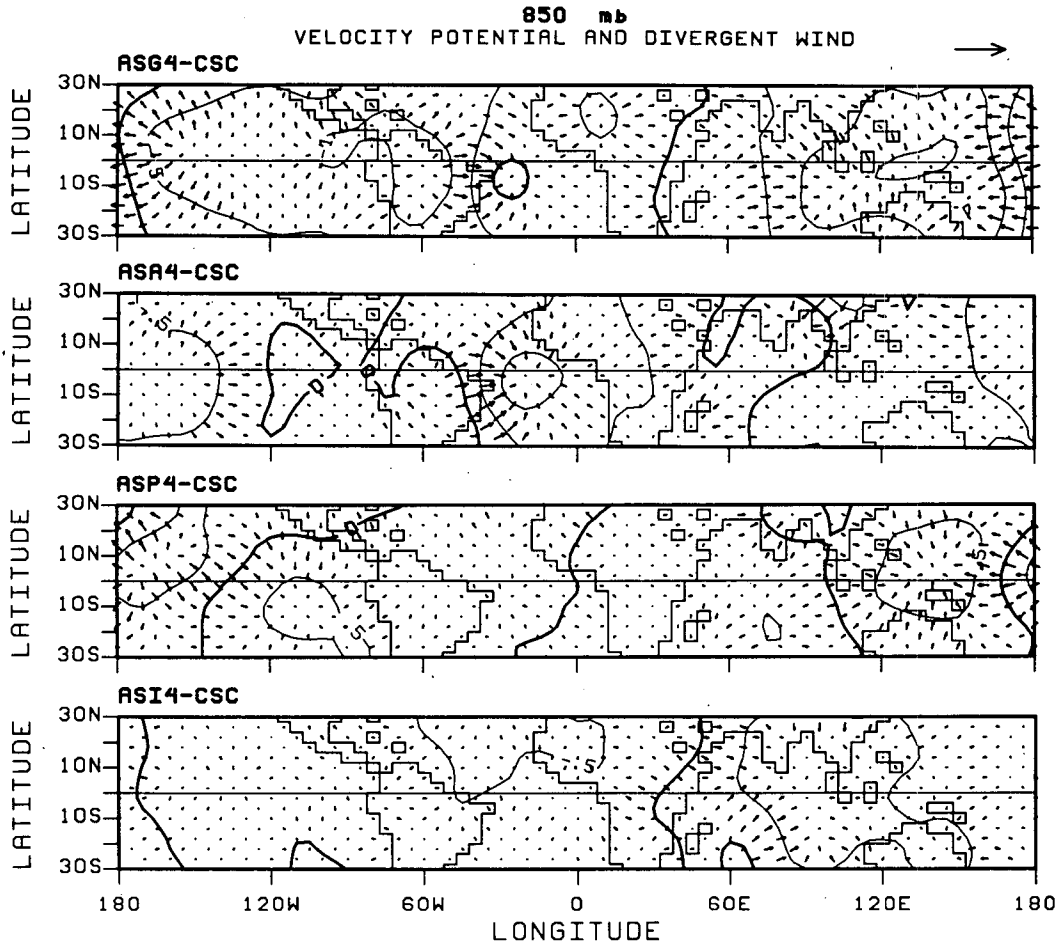


FIG. 6. As in Fig. 2, except for the divergent wind and velocity potential. Reference arrow: 2 m s^{-1} . Contour interval: $0.5 \times 10^6 \text{ m}^2 \text{ s}^{-1}$.

and enhanced precipitation over the western Atlantic south of the equator. There is also enhanced precipitation over the western Indian Ocean north of the equator and scattered regions of decreased precipitation over the western Pacific. The precipitation anomalies in ASA4 are practically confined to the dipole found in ASG4, but the positive component of the dipole is weaker and more diffuse than in ASG4. The increased precipitation near Indonesia obtained in ASP4 is further to the west than in ASG4. Further, the reduction in precipitation over the western Pacific obtained in ASP4 is stronger and better organized than in ASG4. The anomalies obtained in ASI4 show the increased precipitation over the western Indian Ocean found in ASG4. It follows that, except for the western Pacific, the combining of the anomalous precipitation patterns obtained with the SST anomalies confined to a single ocean basin accounts for most major features of the pattern obtained with the global distribution of SST anomalies. We come back to this point later in this paper.

We now focus on the region extending from South America to western Africa. For this region, the results

obtained in ASG4 show that the SST anomalies are associated with a general weakening of the southeast trade winds (see section 4). The weakening is more apparent the further the location is from the African coast. This suggests a scenario for the dipole of reduced-enhanced precipitation in the western part of the region: the negative component over northern Brazil is due to the decreased moisture flux from the Atlantic Ocean into the South American continent; the positive component over the western Atlantic is due to the enhanced convergence of the southeast trade winds carrying moisture over the warmer ocean. To narrow down on this aspect of the problem, we analyze the anomalies in the moisture flux and its convergence. We consider the moisture flux in the entire atmospheric column and in the PBL separately, as in Mechoso et al. (1987). This separation can be easily accomplished for the UCLA GCM, since the variable-depth PBL is the lowest model layer.

The anomalous moisture flux and its convergence for ASG4 are shown in Fig. 8. For the atmospheric column, the anomalous moisture flux along the equator is westerly and strongly divergent over northern Brazil.

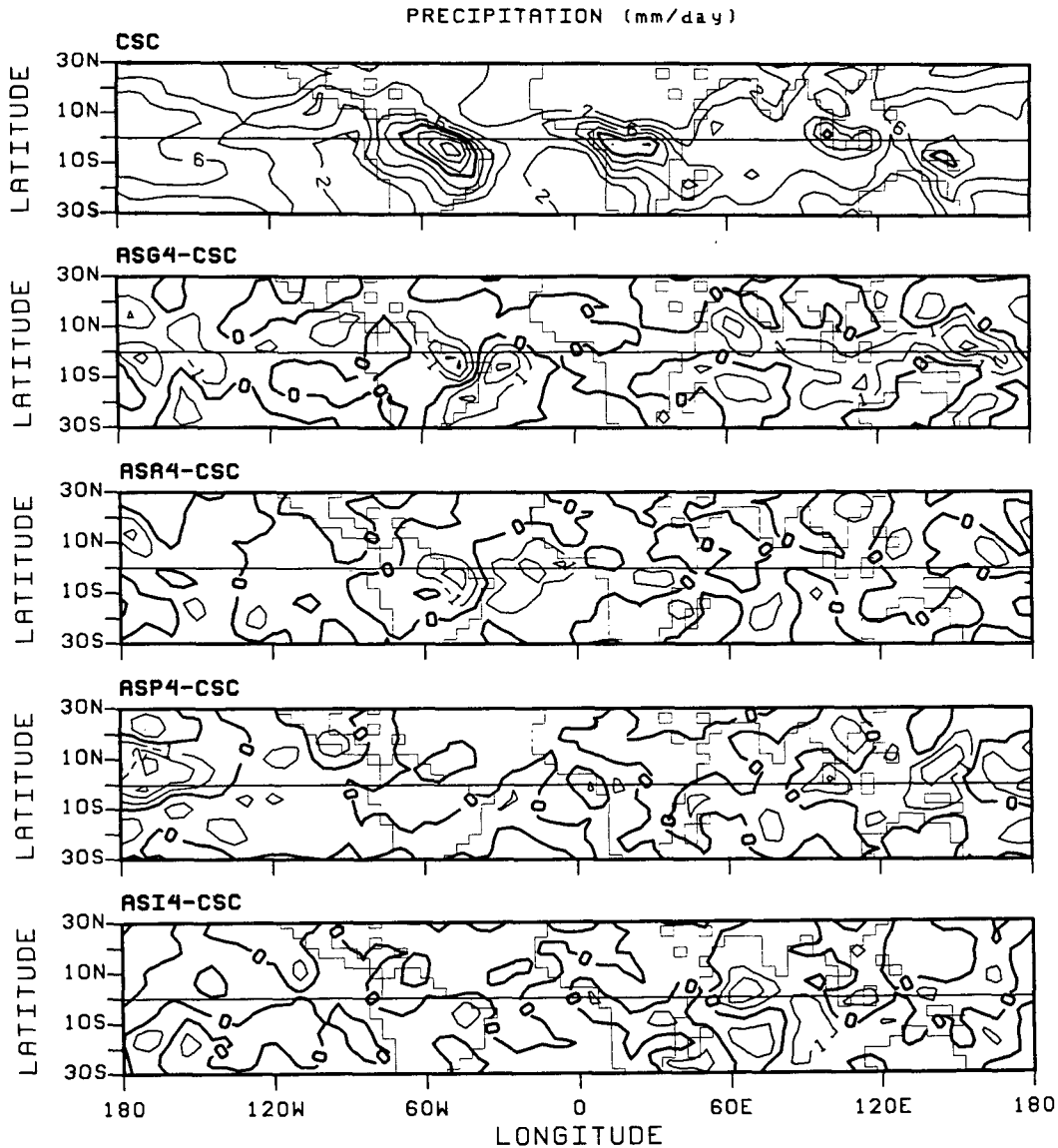


FIG. 7. From top to bottom: NH spring-mean of the climatological precipitation in the control simulation, and of the precipitation anomalies for 1984 obtained in the simulations with the SST anomalies for the Global, Atlantic, Pacific and Indian oceans. Contour interval: 1 mm day⁻¹.

This supports the hypothesis advanced in the previous paragraph concerning the decreased moisture flux over the continent by weaker southeast trade winds. Over the western Atlantic, the moisture flux splits into northern and southern branches. The northward branch, which extends over northern Africa, is almost nonconvergent. The southern branch, which extends along the tropics of the Southern Hemisphere, is strongly convergent over the region of increased precipitation in the western Atlantic (see Fig. 7). The anomalous moisture flux in the PBL is small over the continents and similar, although weaker, to that in the atmospheric column over the oceans. Here, the sign of its convergence and that in the atmospheric column

are in broad agreement. The patterns of the anomalous moisture flux in the atmospheric column and anomalous rotational wind at 850 mb are generally similar (see Fig. 3), particularly over the Southern Hemisphere.

The distributions of the anomalous precipitation and the moisture flux convergence (Figs. 7 and 8, respectively) are strongly similar. This confirms that anomalies in moisture transport, rather than in the in situ evaporation, are generally responsible for the anomalous precipitation. The anomalous precipitation along the coast of Northeast Brazil is not associated with anomalous moisture flux convergence in the PBL. This result is interesting from the modeling point of view,

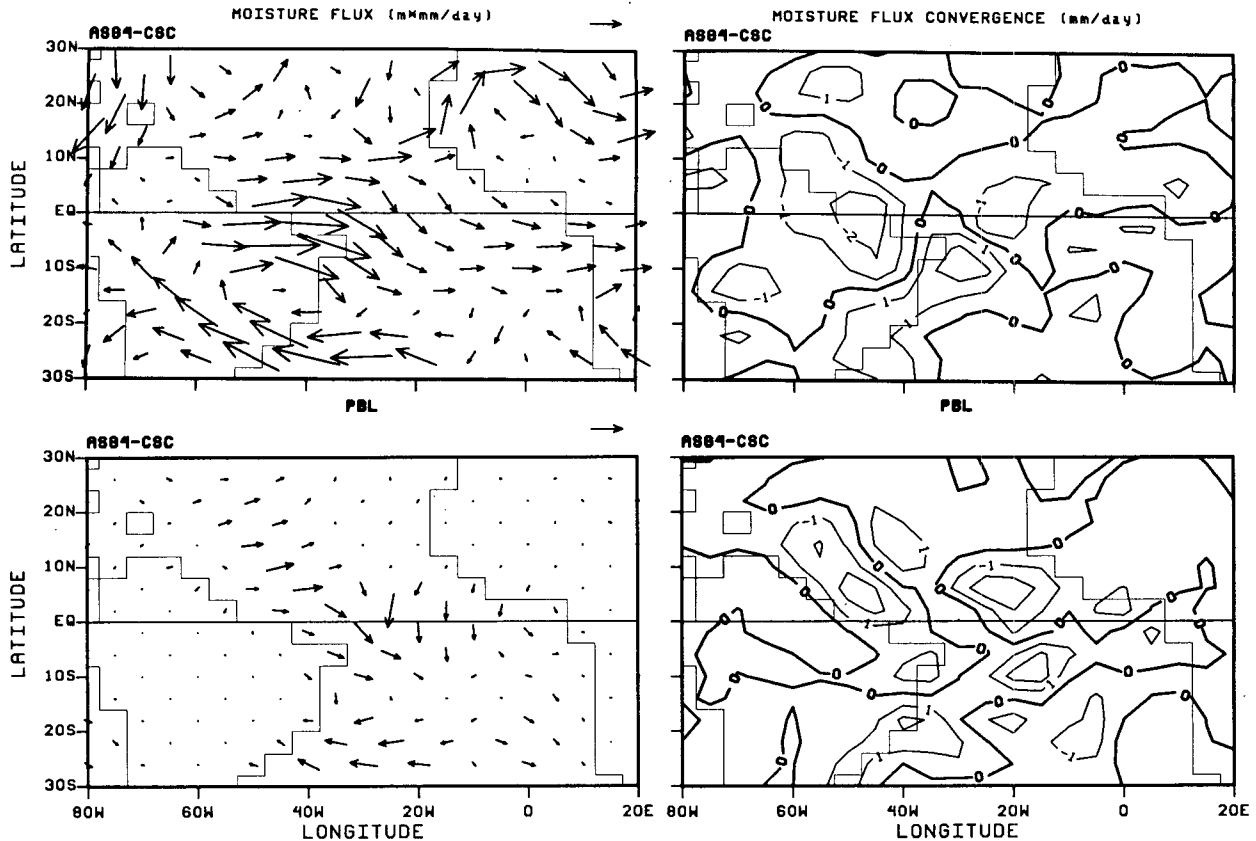


FIG. 8. NH spring-mean for 1984 of the anomalous moisture flux and moisture flux convergence obtained in the simulation with the SST anomalies for the Global Ocean. The bottom row shows the contribution of the PBL. Reference arrow: $2 \times 10^6 \text{ mm day}^{-1}$. Contour interval 1 mm day^{-1} .

since it could not be obtained with a parameterization of precipitation in terms of the PBL fields only. The large reductions in precipitation over northern Brazil and adjacent ocean correspond to the largest anomalous divergences in the region. In this case, the PBL contribution to the anomalous moisture flux convergence dominates over the ocean while that of the free-atmosphere (above the PBL) dominates over land. This suggests that the impact of the SST anomalies on moisture processes is more local in the PBL than in the free-atmosphere. The results shown in Fig. 8 are consistent with the notion that the ITCZ travels further south in years with warm SST anomalies in the tropics of the Southern Hemisphere.

The patterns of anomalous moisture flux and its convergence obtained in ASG3 (see Fig. 9), are significantly different from those in ASG4. For the atmospheric column, ASG3 shows anomalous easterly, weakly convergent fluxes over the equatorial Atlantic. The only strong anomalous convergences in the region are over southeast Brazil corresponding to increased precipitation (see Fig. 5 in ML). Remarkably, the magnitude of the anomalous moisture flux convergence in the atmospheric column over the tropical Atlantic is generally small although in the PBL it can be large.

In this case, therefore, there is weak anomalous precipitation despite large anomalous moisture flux convergence in the PBL due to the tendency toward local cancellation between that convergence and divergence in the free-atmosphere. The anomalies in moisture flux convergence in the PBL are consistent with an anomalous northward displacement of the ITCZ, since there are anomalous convergences north of the equator and divergences over the equator.

For Northeast Brazil, ASG3 shows increased precipitation in an amount comparable with the interannual difference in the control simulation (see Figs. 4 and 5 in ML). In this case, therefore, the results for the Nordeste are inconclusive although the large-scale pattern of the anomalous circulation over the tropical Atlantic Ocean resembles that observed in a year of *seca*, such as 1983.

5. Nonlinearities and local-remote effects in the atmospheric response to SST anomalies

a. Nonlinear response

As was discussed above, the anomalies in the atmospheric circulation obtained with the global distribution of SST anomalies differ in several aspects from

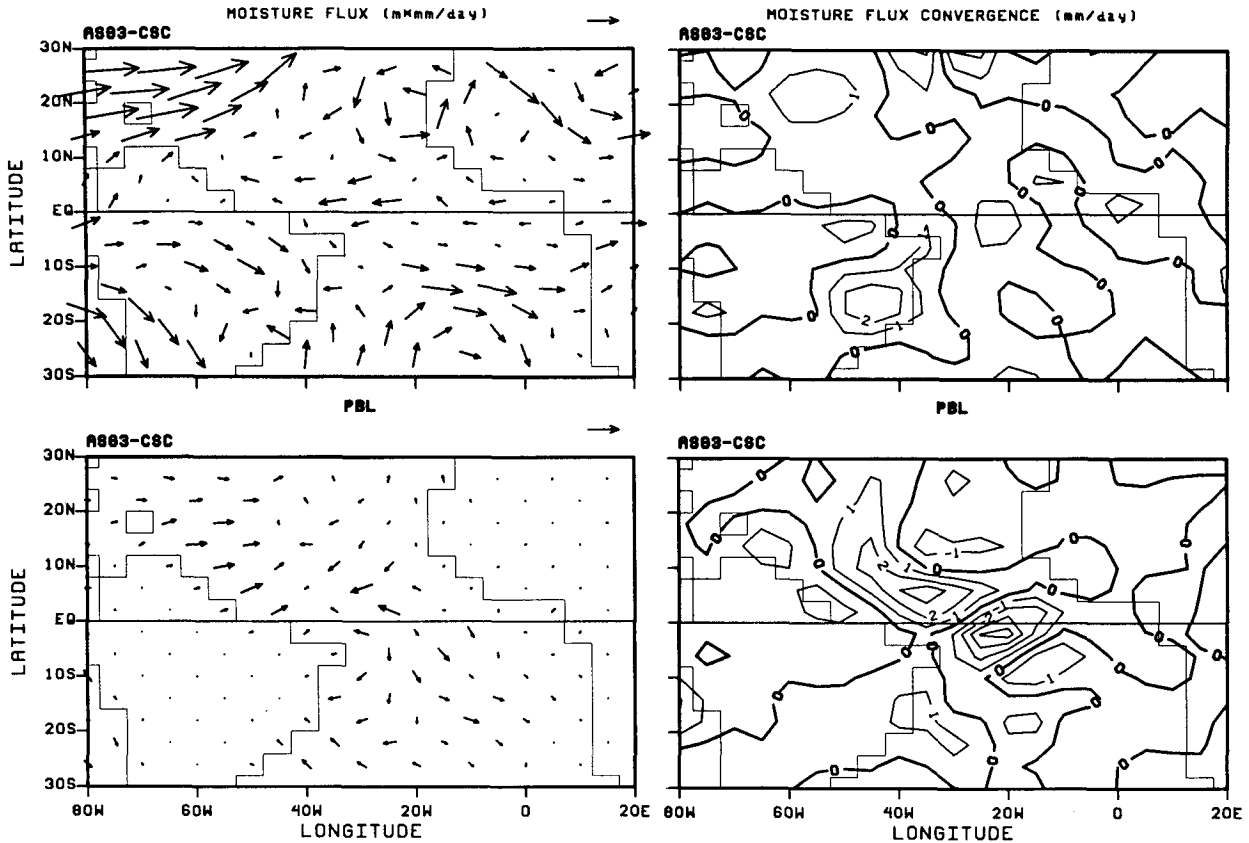


FIG. 9. As in Fig. 8, except for 1983.

the superposition of those obtained with the SST anomalies confined to a single ocean basin. This is illustrated in Fig. 10, which shows the difference between the anomalies obtained in ASG4 and the sum of those in ASA4, ASP4, and ASI4.

Along the equator, the largest differences in Fig. 10 are over the Pacific and western Indian oceans. The easterly differences over the Pacific result from the stronger intensification of the Walker circulation in ASG4 than in any of the other simulations, particularly in ASP4 (see Fig. 3). On the other hand, the westerly

differences over the western Indian Ocean do not result from qualitative differences between the wind anomalies in ASG4 and ASI4. They are primarily a consequence of displacements in latitude of the wind anomalies obtained in these simulations. This variability is not unexpected in the results of the small number of simulations performed for this investigation.

The corresponding difference in anomalous precipitation (see Fig. 11) shows large positive values both east and west of the date line. Here, the precipitation anomalies obtained in ASG4 are larger than the su-

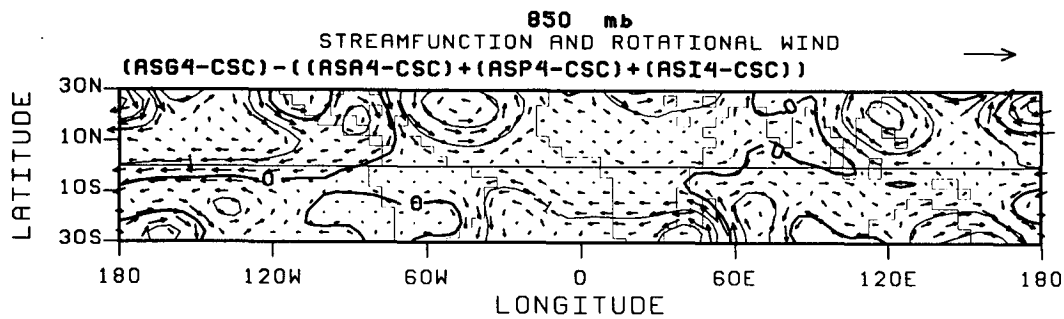


FIG. 10. Difference between the NH spring-mean for 1984 of the rotational wind and streamfunction anomalies obtained in the simulation with the SST anomalies for the Global Ocean, and the sum of those obtained with the SST anomalies confined to a single ocean basin. Units are as in Fig. 3.

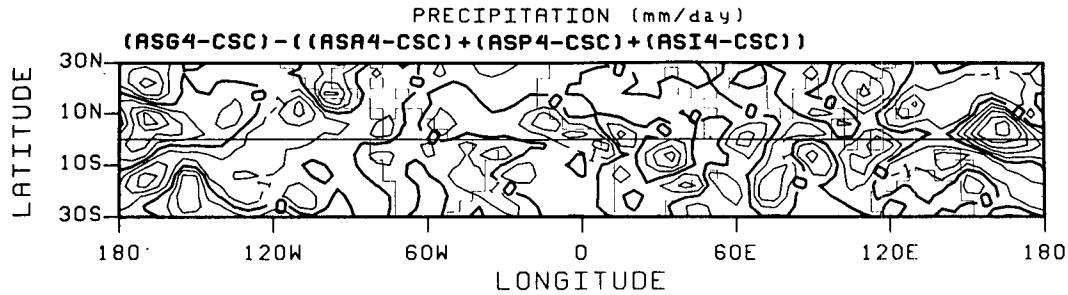


FIG. 11. As in Fig. 10, except for the anomalous precipitation. Units are as in Fig. 7.

position of those obtained with the SST anomalies confined to an ocean basin.

b. Remote effects in the response

Although the 1984 Atlantic event is unusually strong, Fig. 2 shows simultaneous SST anomalies with significant magnitude in the other ocean basins. Their potential importance is compounded by the fact that the geographical extent of the tropical Atlantic is comparable to that of the Indian Ocean and smaller than that of the Pacific Ocean. For the purposes of this study, therefore, it is relevant to analyze the impact of the SST anomalies in the Pacific and Indian oceans on the atmospheric circulation over the Atlantic, particularly on the anomalous precipitation. It is also relevant to analyze the impact of SST anomalies over the Atlantic and Indian oceans on the atmospheric circulation over the Pacific in view of the differences obtained for this region between the simulations with the global and basin distributions of SST anomalies. Neelin (1988) finds that even for highly localized SST anomalies, such as those developing in the Pacific during El Niño, it is misleading to think of the atmospheric response to SST anomalies in terms of a localized effect surrounded by a decay region. The impact of local and remote forcings can be comparable although the former are more intense.

To illustrate the remote response in the precipitation over the Atlantic to the SST anomalies over the Pacific and Indian oceans, we plot in Fig. 12 the sum of the anomalous precipitation in ASP4 and ASI4. Figure 12

suggests that the remote SST anomalies contribute, albeit weakly and by no means crucially, to the dipole found in ASG4 over the northern Brazil–western Atlantic region (see Fig. 7). Here, the sum of the responses in ASP4 and ASI4 is about double the interannual difference in precipitation for the control simulation (see Fig. 5 in ML).

To illustrate the remote response in the rotational wind and streamfunction over the Pacific, we plot in Fig. 13 the sum of the corresponding anomalies obtained in ASA4 and ASI4. Figure 13 shows substantial easterly anomalies extending from the maritime continent to the east of the date line, and weak anomalies over the eastern Pacific. The easterly anomalies obtained in ASG4 over the central Pacific, therefore, are not found by considering separately the local or the remote effects of the SST anomalies (see also Fig. 3). It follows that although the remote effects can be important their superposition to the local effects, in the linear sense, can still fall short of capturing the impact of the global SST anomalies.

6. Diurnal variation of anomalous precipitation

The diurnal variation of insolation is among the radiative effects included in the UCLA GCM. In this section, we study the extent to which the impact of SST anomalies on the atmospheric circulation is modulated by the diurnal cycle. In view of the relatively coarse resolution of the GCM, the discussion is restricted to synoptic and larger scale features: we do not refer to the observed nocturnal maximum in precipi-

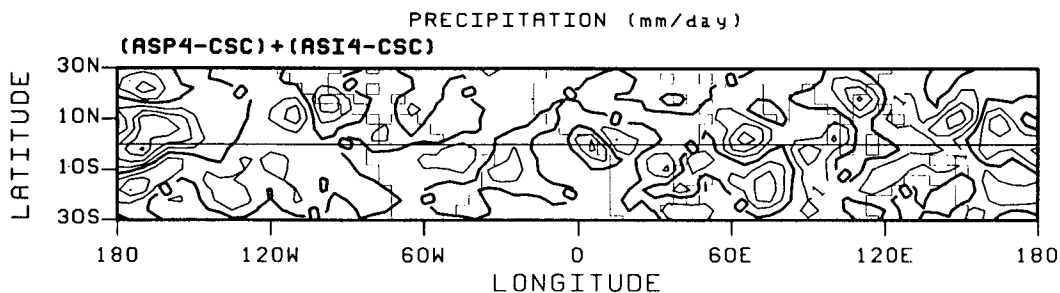


FIG. 12. Sum of the NH spring-mean for 1984 of the anomalous precipitation obtained in the simulations with the SST anomalies confined to the Pacific and Indian oceans. Units are as in Fig. 7.

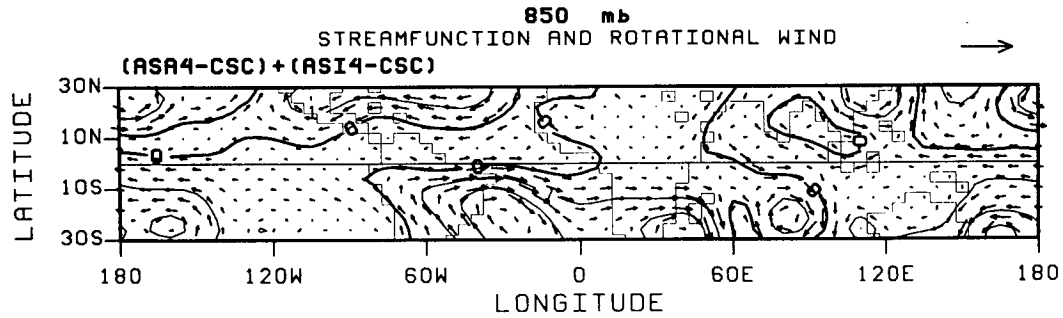


FIG. 13. As in Fig. 12, except for the rotational wind and streamfunction anomalies obtained in the simulations with the SST anomalies confined to the Atlantic and Indian oceans. Units are as in Fig. 3.

tation along the coast of the Nordeste due to the convergence of the mesoscale land-breeze and the trade winds. Nevertheless, the analysis of the diurnal variation in precipitation is relevant since we are interested in anomalies over continental areas in the tropics, where diurnal variations can be large. Suarez et al. (1983) show that the GCM is capable of simulating the diurnally varying continental PBL. We focus on the region between 80°W and 20°E, and take the accumulated precipitation for the periods 1200–0000

UTC and 0000–1200 UTC as representative of daytime and nighttime, respectively. For the Nordeste, in particular, the daytime and nighttime precipitation so defined correspond to those obtained between the local times of 0900–2100 and 2100–0900, respectively.

The NH spring-mean of daytime and nighttime precipitation obtained in the control simulation and anomalous precipitation for 1984 obtained with the global distribution of SST anomalies are shown in Fig. 14. The simulated daytime climatological precipitation

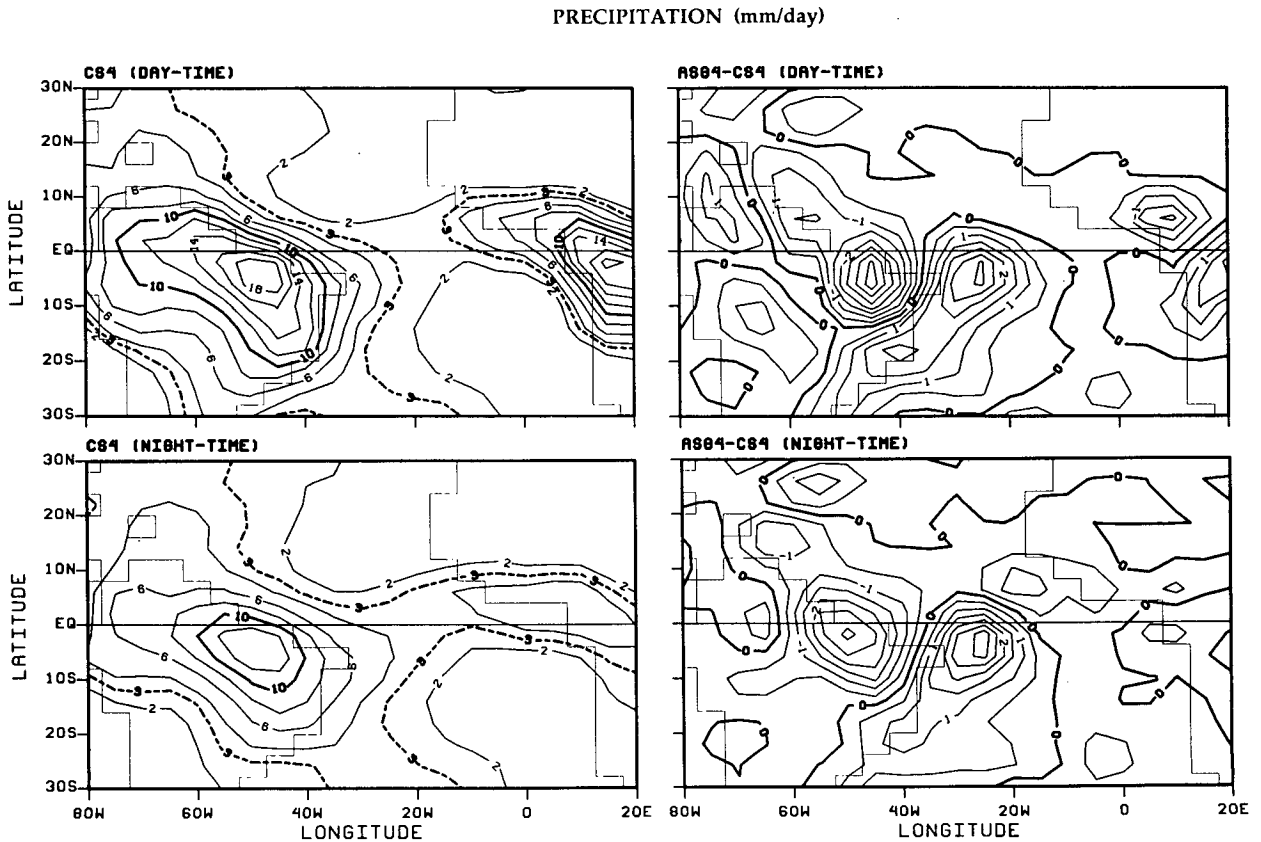


FIG. 14. NH spring-mean of daytime and nighttime climatological precipitation in the control simulation and anomalous precipitation for 1984 obtained in the simulation with the SST anomalies for the Global Ocean. Units are as in Fig. 7.

has local maxima with comparable magnitudes over the continental tropical regions, that for nighttime also peaks over the continents but the magnitudes are significantly weaker than those for daytime, particularly over Africa. As expected, the diurnal variation of precipitation over the ocean is small.

The different impact of the diurnal cycle on the precipitation over South America and Africa can be interpreted as follows. Over South America, precipitation is linked to organized low-level convergence, and the effect of diurnal heating is of secondary importance. Over Africa, on the other hand, low-level convergence is poorly organized and the effect of diurnal heating becomes dominant.

The corresponding results for the anomalous precipitation also show significant differences over the continents. Over South America the anomalies for daytime are stronger than those for nighttime. Over Africa, there are negative anomalies over the western tropical region and positive anomalies over the central equatorial region for daytime and very weak anomalies for nighttime when the precipitation is small. As expected, the precipitation anomalies over the ocean are not significantly affected by the diurnal cycle. Consideration of the diurnal cycle, therefore, seems to be more important for the study of circulation anomalies over Africa than over South America.

7. Conclusions

This is a study of the impact of SST anomalies on the atmospheric circulation over the tropics. We focus on two spring seasons—1984 and 1983—which are characterized in the equatorial Atlantic by intense and large-scale SST anomalies with nearly opposite patterns. In addition, the 1983 period includes the decaying phase of the strongest El Niño on record. Our objectives are twofold: 1) to understand better the mechanisms involved in the link between the anomalies in SST and in rainfall, particularly over northeast Brazil (Nordeste) and 2) to assess the consequences of arbitrarily restricting to a single ocean basin the SST anomalies considered in GCM sensitivity studies.

Our methodology to achieve these objectives is based on performing a comparative analysis of simulations with the UCLA GCM. The simulations are performed with and without observed, time-varying SST anomalies superimposed on an observed time-varying, climatology. The SST anomalies are either global or confined to the Atlantic, Pacific, and Indian oceans. Although we do not perform large ensembles of simulations, our previous work (Mechoso et al. 1987) shows that we can still gain an insight into the tropical response.

The anomalies in the atmospheric circulation simulated for the NH spring of 1984 with the global distribution of SST anomalies are in broad agreement with the observed. At low levels, there are anomalous westerlies over the equatorial Atlantic associated with an

anomalous cyclonic circulation centered over southeast Brazil. There is anomalous low-level moisture flux convergence and enhanced precipitation off the northeast coast of Brazil as the region of strong convection moves east from the continent to the ocean. An anomalous direct overturning is established with air rising over the anomalously warm ocean, and descending over the anomalously cold ocean and adjacent continent, in conceptual agreement with Moura and Shukla (1981). Therefore, in the simulations, the apparent north-south displacement of the ITCZ results from an anomalous east-west circulation in the subtropics of the Southern Hemisphere. In addition, the trade winds are stronger than normal over the Pacific.

These results suggest that the warm SST anomalies in the southern tropical Atlantic result in increased convection over the western part of the region and adjacent continental areas, including the Nordeste. This increase is associated with a weakening of the trade winds over inland areas downstream of the enhanced convection. The increased precipitation develops despite a general decrease of westward moisture flux due to the weakening of the southeast trade winds over the ocean.

Philander (1986) questions whether the strengthening of the trade winds observed over the Pacific in the NH spring of 1984 is a consequence of the cold SST anomalies in the Pacific Ocean. The results obtained in our study suggest that this is not so. In the simulation performed with the SST anomalies confined to the Pacific Ocean, there is only a weak strengthening of the trade winds over part of the western Pacific and rather strong westerly anomalies over the maritime continent. In fact, strong anomalous trades over the Pacific extending east of the date line are not obtained in any of the simulations with the SST anomalies confined to a single ocean basin. On the other hand, the simulated anomalies over the tropical Atlantic and Indian oceans can be approximately obtained with the SST anomalies confined to the corresponding basins. Based on these considerations, we conclude that the local atmospheric response to SST anomalies can be sensitive to remote features in the global SST anomaly field, even when the component of this field in the corresponding ocean basin is significantly strong. These results are supportive of those obtained by Neelin (1988) in the idealized context of a simple model for surface stress and low-level flow. Neelin's model clarifies that the impact of local and remote forcings can be comparable, although the former are more intense.

That the simulated impact on the atmospheric circulation over an ocean basin can significantly depend on the geographical extent covered by the prescribed SST anomalies is a finding with far reaching consequences. First, it raises questions on the mechanisms at work in the teleconnection between regions of large-scale convection. Second, it seriously questions the validity of parameterizations for anomalous precipitation based on local SST anomalies. Third, it questions the

validity of approaches to the air-sea interaction problem based on modeling a partial region of the ocean. In such approaches, anomalies generated over a non-modeled ocean region cannot affect the local SST and feedback on the region where air-sea interaction is allowed.

Acknowledgments. It is a pleasure to thank two anonymous reviewers for their thorough job with the original version of this manuscript. Special thanks are due to Mr. M. Fisher for useful comments and to Messrs. A. Quintanar and M. Picazo for technical assistance. Ms. C. Wong typed the manuscript. This research was supported by the National Science Foundation under Grant ATM-85-17916. Integrations of the UCLA GCM were performed at the National Center for Atmospheric Research and San Diego Supercomputer Center.

APPENDIX

Sensitivity to Initial and Boundary Condition

There are substantial differences between the wind anomalies obtained in ASG4 and ASP4. To explore the sensitivity of these results to the starting dates of the simulation, we perform two additional pairs of anomaly simulations. The simulations in each pair start from the same initial conditions. These correspond to 0000 UTC 1 November 1983 and 1 January 1984 in the control. One of the simulations uses the global distribution of SST anomalies (as in ASG4) while the other uses the SST anomalies confined to the Pacific Ocean (as in ASP4). The results for the NH spring-mean rotational wind and streamfunction anomalies at 850 mb are shown in Fig. 15.

Comparison of Figs. 3 and 15 reveals a number of common features in the equatorial region: 1) all sim-

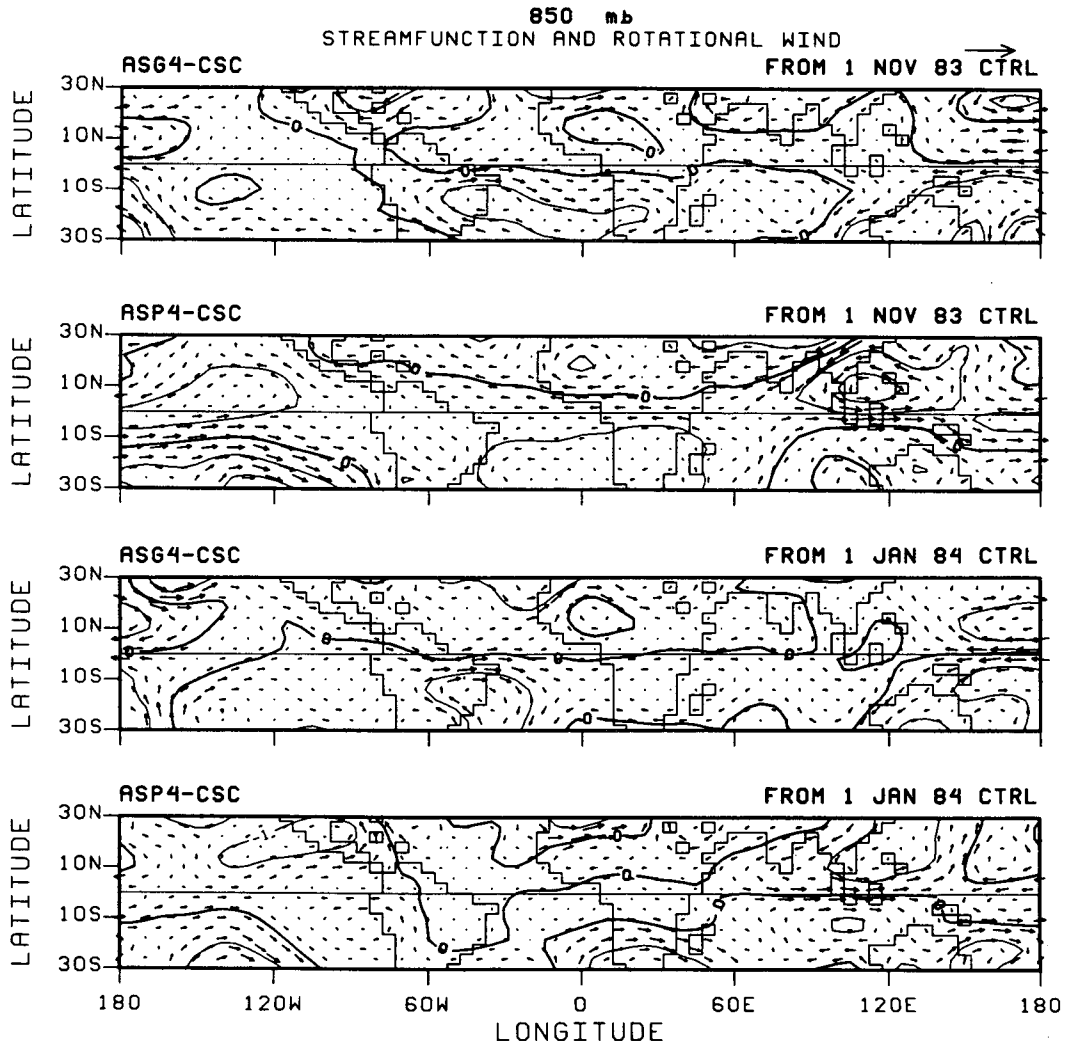


FIG. 15. As in Fig. 3, except for the simulations with the SST anomalies for the Global and Pacific oceans from initial conditions corresponding to 0000 UTC 1 November 1983 and 1 January 1984 in the control.

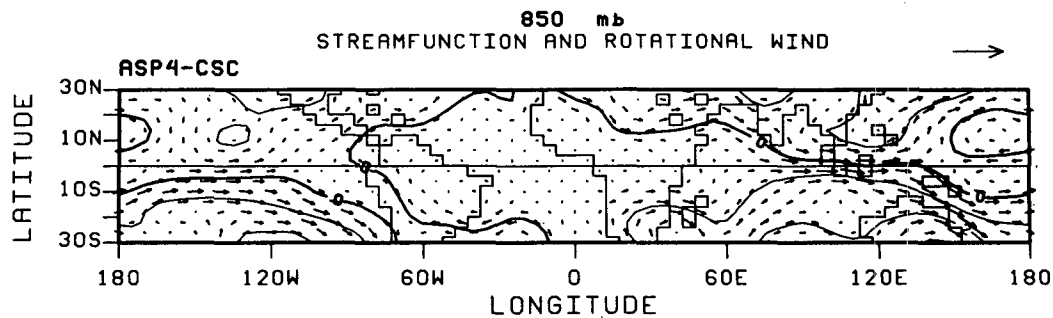


FIG. 16. As in Fig. 3, except for the simulation with the SST anomalies confined to the Pacific Ocean and such that anomalies at the boundaries decay linearly outward over a distance equivalent to three GCM grid points in the zonal direction.

ulations with the SST anomalies in the global domain show anomalous westerlies over the Atlantic and Indian oceans, as well as over South America and Africa, and strong easterlies over the western Pacific extending east of the date line; and 2) all simulations with the SST anomalies confined to the Pacific Ocean show strong westerlies over the maritime continent, and weak easterlies and westerlies over the western and central Pacific, respectively. Figures 3 and 15 show that, east of the date line, the anomalous easterlies over the equatorial Pacific obtained in simulations with the global distribution of SST anomalies extend to a distance that is sensitive to the starting date.

Another matter of concern is the effect that discontinuities in the SST anomalies across the arbitrary boundaries of the ocean basins can have on the results (see Fig. 1). In particular, part of the boundary between the Pacific and Indian oceans is in the tropics. To address this concern, we repeat ASP4 after allowing the SST anomalies at the boundaries of the Pacific to decay linearly outward over a distance equivalent to three GCM grid points in the zonal direction. The new results for the NH spring-mean of the rotational wind and streamfunction anomalies at 850 mb are shown in Fig. 16. It is apparent that the discontinuities at the boundaries do not seem to have a major impact on the atmospheric response to the SST anomalies in the basin.

It is pertinent to mention, in the context of this paper, that the dipole of reduced precipitation over northern Brazil and enhanced precipitation over the western Atlantic south of the equator (see Fig. 7) is obtained in all simulations with the global distribution of SST anomalies.

REFERENCES

- Hasternath, S., 1978: On modes of tropical circulation and climate anomalies. *J. Atmos. Sci.*, **35**, 2222–2231.
- , 1984: Predictability of north-east Brazil droughts. *Nature*, **307**, 531–533.
- , and L. Heller, 1976: Dynamics of climatic hazards in Northeast Brazil. *Quart. J. Roy. Meteor. Soc.*, **103**, 77–92.
- Horel, J. D., V. E. Kousky and M. T. Kagano, 1986: Atmospheric conditions in the Atlantic sector during spring 1983 and 1984. *Nature*, **328**, 590–596.
- Kousky, V., 1979: Frontal influences on Northeast Brazil. *Mon. Wea. Rev.*, **107**, 1140–1153.
- , and P. S. Chu, 1978: Fluctuations in annual rainfall for Northeast Brazil. *J. Meteor. Soc. Jpn.*, **56**, 457–465.
- Lamb, P. J., R. A. Pepler and S. Hastenrath, 1986: Interannual variability in the tropical Atlantic. *Nature*, **322**, 238–240.
- Markham, C., and D. McLain, 1977: Sea surface temperature related to rain in Ceara, Northeast Brazil. *Nature*, **265**, 320–323.
- Mechoso, C. R., and S. W. Lyons, 1988: On the atmospheric response to SST anomalies associated with the Atlantic warm event during 1984. *J. Climate*, **1**, 422–428.
- , A. Kitoh, S. Moorthi and A. Arakawa, 1987: Numerical simulations of the atmospheric response to a sea surface temperature anomaly over the equatorial eastern Pacific Ocean. *Mon. Wea. Rev.*, **115**, 2936–2956.
- Moura, A. D., and J. Shukla, 1981: On the dynamics of droughts in Northeast Brazil: Observations, theory and numerical experiments with a general circulation model. *J. Atmos. Sci.*, **38**, 2653–2675.
- Neelin, J. D., 1988: A simple model for surface stress and low-level flow in the tropical atmosphere. *Quart. J. Roy. Meteor. Soc.*, **114**, 747–770.
- Philander, S. G. H., 1986: Unusual conditions in the tropical Atlantic Ocean in 1984. *Nature*, **322**, 236–238.
- Rasmusson, E. M., and T. H. Carpenter, 1982: Variations in tropical sea surface temperature anomalies. *Mon. Wea. Rev.*, **110**, 354–384.
- Ratisbona, L. R., 1976: The Climate of Brazil. *Climates of Central and South America. World Survey of Climatology*, Vol. 12. Elsevier, 523 pp.
- Serra, A., and L. Ratisbona, 1942: As massas de ar da America do Sul. Servico de Meteorologia, Ministerio da Agricultura, 137 pp.
- Servain, J., and M. Seva, 1987: On relationships between tropical Atlantic sea surface temperature, wind stress and regional precipitation indices: 1964–1984. *Ocean-Air Interactions*, **1**, 183–190.
- Suarez, M. J., A. Arakawa and D. A. Randall, 1983: The parameterization of the planetary boundary layer in the UCLA general circulation model: Formulation and results. *Mon. Wea. Rev.*, **111**, 2224–2243.